

Studies of fast particle modes in ASDEX Upgrade using reflectometry and comparison with theoretical prediction

S.da Graça¹, G.D.Conway², P.Lauber², M.Maraschek², D.Borba¹, S.Guenter²,
L.Cupido¹, K.Sassenberg³, F.Serra¹, M.E.Manso¹, the CFN reflectometry group¹ and
the ASDEX Upgrade Team²

¹ *Centro de Fusão Nuclear, Associação EURATOM / IST, Instituto Superior Técnico,
Av. Rovisco Pais, P-1049-001 Lisboa, Portugal*

² *Max-Planck-Institut fuer Plasmaphysik, Garching, Euratom Association, Germany*

³ *Physics Department, University College Cork, Cork, Ireland*

1. Introduction

Alfvén eigenmode instabilities, such as toroidicity induced Alfvén eigenmodes (TAEs) and Alfvén cascades (ACs) have attracted much attention due to their potential to expel α particles with resulting damage to the first wall components of a reactor, as well as reducing the efficiency of plasma self-heating. In ASDEX Upgrade a heterodyne fast frequency hopping reflectometry system allows probing of different density (n_e) cutoff layers from the low field side during the same discharge. In this paper, comparison between experimental radial eigenfunction for $n = 4$ TAE mode and numerical predictions (LIGKA [1] and CASTOR) is shown. First results on the localization of ACs are presented.

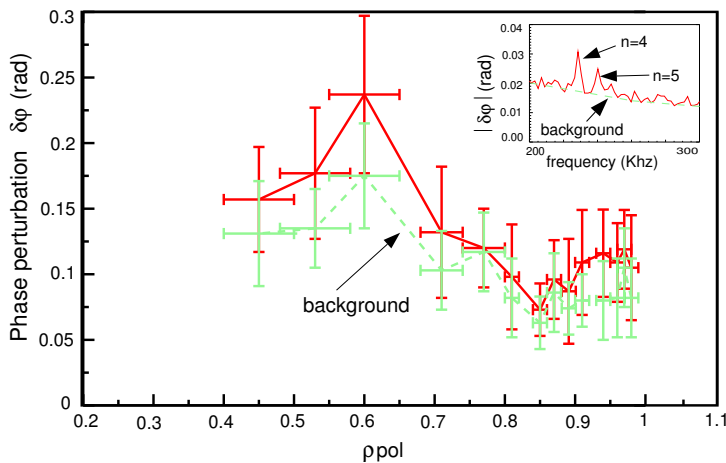


Figure 1: Reflectometer phase perturbation profile for $n = 4$ TAE, background profile and phase spectrum (insert) for shot #21007.

most toroidally located Mirnov coil signal to give the coherence and the cross-phase of the mode vs radial position; (2) the δn_e fluctuation level at each cutoff position is estimated using the 1D Geometric optics (GO) model [3]: $\delta\phi = (4\pi/\lambda) (\delta n/n) \nabla n^{-1}$, where

2. Technique

In ASDEX Upgrade, a dual O-mode channel (Q-band: 33-49.2GHz and V-band: 49-72GHz) fast frequency hopping reflectometer with I-Q detection [2] is dedicated to n_e fluctuation measurements. To obtain the radial structure of coherent modes two analysis techniques were used: (1) each cutoff signal is correlated with the near-

λ is the vacuum wavelength of the probing wave. This model is strictly only valid for long fluctuation wavelength and small amplitude fluctuations. In both analysis methods the n_e profile is needed to give the radial cutoff position. Here, a fitted profile is obtained using Thomson Scattering (TS), Lithium Beam (LID) and reflectometry data.

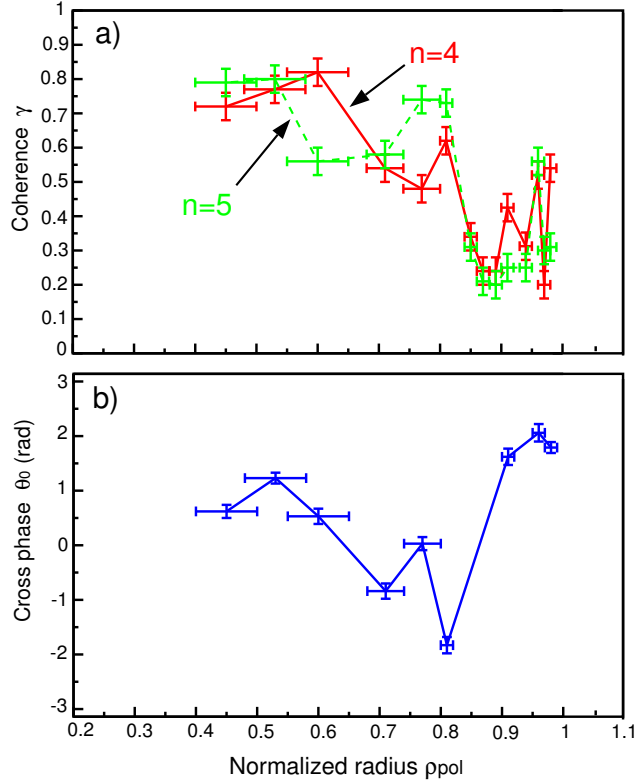


Figure 2: Coherence analysis: (a) Coherence profile for $n = 4$ and $n = 5$ TAE modes, (b) Cross-phase profile for $n = 4$ TAE mode for shot #21007.

4. Phase perturbation analysis

In this analysis, the discharge #21007 with 4.5 MW pure ICRH, $B_T = -2$ T, $I_p = 1$ MA and $\bar{n}_e \approx 3.6 \times 10^{19} \text{ m}^{-3}$ was used. The reflectometer frequency pattern is 11 steps of 15 ms. Figure 1 shows the phase spectrum and the radial profile of $\delta\varphi(f)$ for the $n = 4$ TAE mode. The $\delta\varphi(f)$ for each TAE mode is obtained by integrating the phase spectrum over 10 kHz around each peak and calculating the average value and standard deviation for a time window of 10 ms. The maximum peak in $\delta\varphi(f)$ is around $\rho_{pol} = 0.6 \pm 0.05$ with a less pronounced secondary peak at the edge. The background fluctuation level at each radial position is also

considered by integrating the phase spectrum over 10 kHz at two frequency positions, just before the first peak and just after the last peak between 260 kHz and 270 kHz, the average is calculated as well as the standard deviation. The $\delta n_e/n_e$ can be calculated using the 1D GO model, however, the error bars in $\delta n_e/n_e$ are increased due to ∇n_e . The $\delta n_e/n_e$ radial profile have peak amplitudes of $\delta n_e/n_e = 2.5 \times 10^{-4}$ (0.025 %) at the edge and $\delta n_e/n_e = 0.41 \times 10^{-4}$ (0.0041 %) in the core.

5. Coherence analysis

For the same discharge, #21007, the coherence and cross-phase analysis technique is applied to determine the radial structure of $n = 4$ TAE mode. The significance level of the coherence is $\gamma_0 = 0.16$, defined by the number of spectral averages and window lengths, in this case 10 ms and $N_{av} = 39$. Figure 2(a) shows the coherence radial profiles for the $n = 4$ and $n = 5$ TAE modes. The corresponding θ_0 radial profile giving

the sign of the radial displacement is shown in figure 2(b) for the $n = 4$ TAE mode.

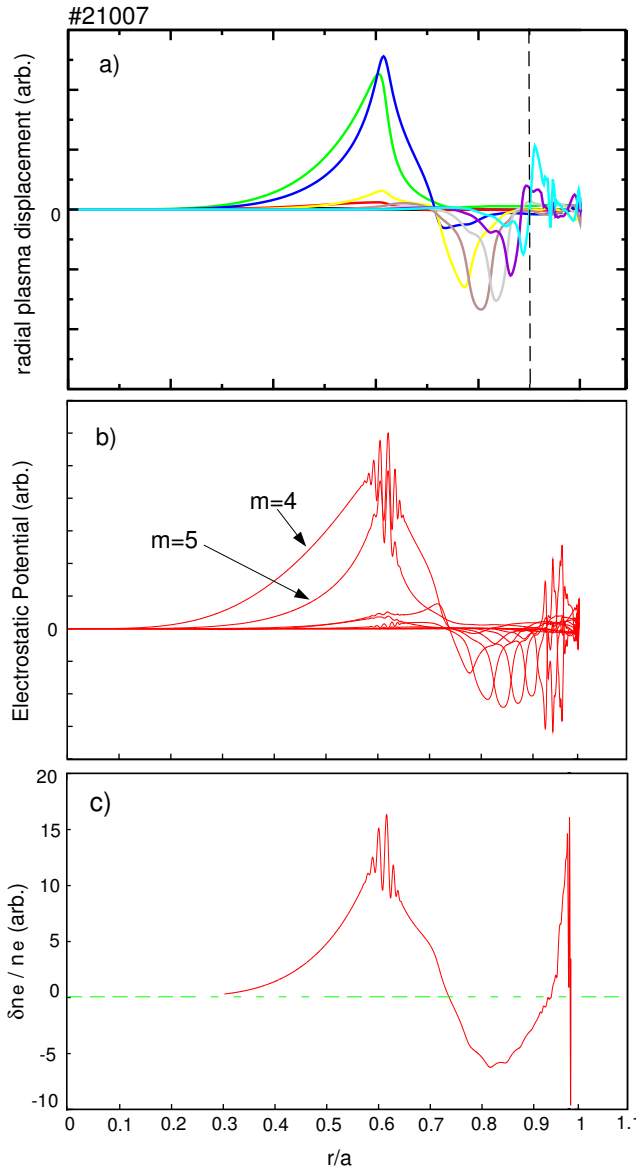


Figure 3: Simulated radial eigenfunction of (a) radial plasma displacement, (b) electrostatic potential and (c) $\delta n_e / n_e$ for $n = 4$ TAE mode from CASTOR and LIGKA codes.

in general very good. From the coherence and cross-phase analysis (figure 2), the relative amplitude as well as the sign of the radial eigenfunction are reproduced. The reflectometer phase magnitude profile in figure 1 is also in good agreement with simulation, although unfortunately no information on the sign of the radial eigenfunction is available from the phase magnitude technique. The LIGKA code also predicts continuum damping at the edge which are characteristic of closed gaps [4].

6. Alfvén Cascades

In ASDEX Upgrade, modes with upward frequency sweeping are observed in the early

The θ_0 is the cross-phase value corrected for the toroidal displacement between the reflectometer antenna and Mirnov coil positions and only values with a coherence greater than 0.4 are included in order to avoid noise effects. From the coherence and cross-phase profiles it is clear that a node exists at $\rho_{pol} = 0.8 \pm 0.02$. The main contribution of the mode is localized in the core with a secondary peak at the edge. The maximum peak is around $\rho_{pol} = 0.6$ and $\rho_{pol} = 0.55$ for $n = 4$ and $n = 5$ TAE modes respectively. The radial structure appears to be consistent with the global TAE mode structure which have a radial width extending over a wide region.

6. Simulations

The CASTOR code is a resistive MHD code which gives only radial eigenfunction in the core while the linear gyrokinetic LIGKA code reproduces radial structure of TAEs from edge to core. The agreement between simulation in figure 3 and experimental results is in

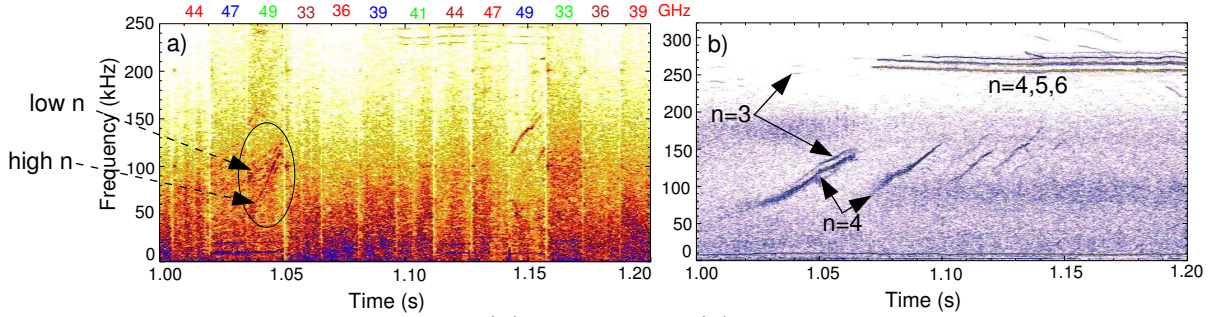


Figure 4: Shot #20398 (a) FLQ-I and (b) magnetic spectrograms.

phase of some discharges with ICRH power ramp-up and I_p constant. For example, in shot #20398 both magnetic and reflectometry data exhibit these modes between 1 – 1.2 s, as shown in the spectrograms in figure 4. At $t = 1.32$ s a sawtooth crash occurs, indicating that q_{min} is decreasing in time. The fast frequency hopping reflectometers were configured with a data sample rate of 500 kHz, however, in this case the aliasing effect allows the estimation of the radial extent of TAEs modes, $\rho_{pol} \approx 0.35 - 0.68 (\pm 0.05)$ using TS density profiles. The chirping modes are core localized with $\rho_{pol} \approx 0.2 - 0.4 (\pm 0.05)$. In both the magnetic and reflectometry measurements the ACs rise until around 150 kHz and stop before the TAE frequency. The slope of the frequency sweeping also varies in time, which is not common in standard ACs observed in other tokamaks. The starting frequency of these chirping modes is below the geodesic frequency. Furthermore, the $n = 4$ AC and TAE are present at the same time suggesting that these non-standard ACs are possibly created by the coupling to the sound branches [5].

7. Discussion and conclusions

The radial structure of $n = 4$ TAE mode was obtained using two different techniques: coherence and phase perturbation analysis. The coherence analysis gives the relative amplitude as well as the sign of the radial eigenfunction. The phase perturbation technique gives the $\delta n_e/n_e$ amplitude induced by $n = 4$ TAE mode. These two techniques show good agreement with simulations.

Acknowledgements: This work has been carried out in the frame of the Contract of Association between the European Community and IST and has received financial support from Fundação para a Ciência e a Tecnologia (FCT). The content of publication is the sole responsibility of the authors and it does not necessarily the views of the Commission of the European Union or FCT or their services.

- [1] Lauber Ph *et al.* 2005 *Phys. Plasmas* **12** 122501, [2] L.Cupido *et al.*, *Rev. Sci. Instrum.* **77**, 10E925 (2006), [3] N.Bretz, *Phys. Fluids B* **4**, 2414 (1992), [4] Guenter S *et al.* 2006 submitted to *Nucl. Fusion*, [5] Lauber Ph *et al.* 2006 *AIP Conf. Proc.* **871** 147